

DESIGN OF DOUBLE- AND MULTI-BEND ACHROMAT LATTICES WITH LARGE DYNAMIC APERTURE AND APPROXIMATE INVARIANTS*

Y. Li[†], R. Rainer, V. Smalyuk, Brookhaven National Lab, Upton, NY, USA
K. Hwang, C. Mitchell, R. Ryne, Lawrence Berkeley National Lab, Berkeley, CA, USA

Abstract

A numerical method to design nonlinear double- and multi-bend achromat (DBA and MBA) lattices with approximate invariants of motion is described. The search for such nonlinear lattices is motivated by Fermilab's Integrable Optics Test Accelerator (IOTA), whose design is based on an integrable Hamiltonian system with two invariants of motion. While it may not be possible to design an achromatic lattice for a dedicated synchrotron light source storage ring with one or more exact invariants of motion, it is possible to tune the sextupoles and octupoles in existing DBA and MBA lattices to produce approximate invariants. In our procedure, the lattice is tuned while minimizing the turn-by-turn fluctuations of the Courant-Snyder actions J_x and J_y at several distinct amplitudes, while simultaneously minimizing diffusion of the on-energy betatron tunes. The resulting lattices share some important features with integrable ones, such as a large dynamic aperture, trajectories confined to invariant tori, robustness to resonances and errors, and a large amplitude-dependent tune-spread.

INTRODUCTION

The Integrable Optics Test Accelerator (IOTA) [1], whose design is based on an integrable Hamiltonian system with two invariants of motion [2, 3], paves the way for a new class of highly nonlinear storage rings. Experiments using a lattice design with one invariant of motion have also been performed, both at IOTA and in the University of Maryland Electron Ring (UMER) [4]. In each case, the lattice is tuned to provide one or more analytically known invariants of motion, resulting in a dynamic aperture (DA) that is large and robust to the presence of resonances.

The storage rings used as dedicated synchrotron light sources are designed in a different way: a linear achromat lattice with a desired beam emittance is designed first, and then the nonlinear dynamics is optimized with sextupoles and/or octupoles. The nonlinear magnets are often tuned to control the low order resonance driving terms of the one-turn map [5] in order to obtain sufficient dynamic aperture. Under these conditions it is generally difficult, if not impossible, to optimize the nonlinear dynamics to produce a one-turn map with one or more exact invariants. However, it is sometimes possible to produce approximate invariants, or quasi-invariants (QI), in these achromat lattices. This paper describes a procedure for designing near-integrable double-bend achromat (DBA) and multi-bend achromat (MBA) lat-

tices with two QI. The motivation for constructing such lattices is that, although they are not completely integrable, the DA is large and robust to the presence of resonances. Like nonlinear lattices such as IOTA, these lattices have a large amplitude-dependent betatron tune-spread which can increase instability and space charge thresholds due to improved Landau damping [6, 7]. This research was also motivated by related studies such as the square matrix method [8] and the constant Courant-Snyder invariant method [9, 10].

LATTICE DESIGN PROCEDURE

By ignoring radiation and longitudinal acceleration, a charged particle's transverse motion in a storage ring is a 4-dimensional Hamiltonian system, described by a symplectic one-turn map \mathcal{M} . If we let the canonical coordinates of the system be denoted $z = (x, p_x; y, p_y)$, a quantity $f(z)$ is an invariant of the map \mathcal{M} if:

$$f(\mathcal{M}(z)) = f(z). \quad (1)$$

If two such invariants f_i , ($i = 1, 2$) exist, if they are independent:

$$\nabla f_1 \times \nabla f_2 \neq 0, \quad (2)$$

and if they Poisson-commute:

$$\begin{aligned} [f_1, f_2] &= \left(\frac{\partial f_1}{\partial x} \frac{\partial f_2}{\partial p_x} - \frac{\partial f_1}{\partial p_x} \frac{\partial f_2}{\partial x} \right) \\ &+ \left(\frac{\partial f_1}{\partial y} \frac{\partial f_2}{\partial p_y} - \frac{\partial f_1}{\partial p_y} \frac{\partial f_2}{\partial y} \right) = 0, \end{aligned} \quad (3)$$

the lattice is Liouville integrable [11, 12]. The behavior of trajectories for a completely integrable system is well-known, i.e., all its trajectories are confined to tori with well-defined and stable tunes.

When the map \mathcal{M} is linear and uncoupled, the Courant-Snyder actions J_x and J_y form the most commonly-used Poisson commuting pair of invariants, where:

$$J_x = \frac{1}{2}(\bar{x}^2 + \bar{p}_x^2) = \frac{1}{2}(\gamma_x x^2 + 2\alpha_x x p_x + \beta_x p_x^2), \quad (4)$$

in the horizontal plane, with a similar expression for J_y . Here the normalized coordinates \bar{x} and \bar{p}_x are given by:

$$\begin{bmatrix} \bar{x} \\ \bar{p}_x \end{bmatrix} = \begin{bmatrix} \frac{1}{\sqrt{\beta_x}} & 0 \\ \frac{\alpha_x}{\sqrt{\beta_x}} & \sqrt{\beta_x} \end{bmatrix} \begin{bmatrix} x \\ p_x \end{bmatrix}, \quad (5)$$

where α_x , β_x , and γ_x are the horizontal Twiss parameters [13] at the longitudinal location where the Poincaré section is observed. The canonical action-angle coordinates

* Work supported by the U.S. DoE under Contract No. DE-SC0012704 (BNL) and DE-AC02-05CH11231 (LBNL).

[†] yli@bnl.gov

are $(\Phi_x, J_x, \Phi_y, J_y)$, where $\Phi_{x,y}$ denotes the betatron phase in each plane, and the one-turn map is determined by the phase advance completed in a single revolution:

$$\begin{aligned} \phi_x &= \Phi_{x,i+1} - \Phi_{x,i} \\ &= -\arctan\left(\frac{\bar{p}_{x,i+1}}{\bar{x}_{i+1}}\right) + \arctan\left(\frac{\bar{p}_{x,i}}{\bar{x}_i}\right) + k \cdot 2\pi, \end{aligned}$$

with a similar expression for ϕ_y . Here k is the integer part of the betatron tune. The phase advance values ϕ_x, ϕ_y are independent of the actions J_x and J_y .

In a realistic storage ring, once the linear lattice and the nonlinear magnet locations are fixed, the one-turn map \mathcal{M} depends on the nonlinear magnet strengths K_i , with $i \geq 2$. It is difficult, if not impossible, to tune the K_i so that \mathcal{M} possesses even one exact invariant. However, we can imitate the linear case by constructing a nonlinear system in which the Courant-Snyder actions J_x, J_y form a pair of approximate invariants, as illustrated in Fig. 1. Unlike the linear case, however, the phase advance values ϕ_x and ϕ_y can depend on the actions J_x and J_y .

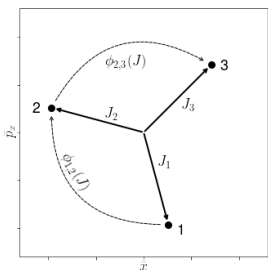


Figure 1: Schematic illustration of a rotating trajectory observed at a Pioncaré section with normalized coordinates (\bar{x}, \bar{p}_x) . The fluctuations of the action J_x and phase advance ϕ_x , in multiple-turn tracking simulations are the objectives to be minimized. A similar picture applied in the vertical plane.

The procedure is as follows. To optimize the behavior of the Courant-Snyder action J_x within the available DA, multiple particles with different values of $J_{x,0}$ are launched. Element-by-element tracking of this set of particles is used to compute the turn-by-turn evolution of J_x . The tracking is implemented with a kick-drift symplectic integrator [14], to preserve the geometry of the Hamiltonian system. The available nonlinear knobs are simultaneously tuned to minimize the turn-by-turn fluctuations of J_x for each particle, as illustrated the left subplot in Fig. 2.

At the same time, we minimize the turn-to-turn variations of the horizontal phase advance. Instead of directly calculating ϕ_x , the turn-to-turn evolution of $\bar{x} \pm i\bar{p}_x$ [15] was analyzed in the frequency domain. One reason for using such a spectral method is to determine whether the fractional tune is below or above the half integer. The amplitudes of the two leading harmonics were computed utilizing the Numerical Analysis of Fundamental Frequencies (NAFF)

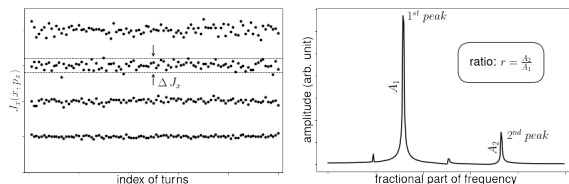


Figure 2: Schematic illustration of (1) the fluctuation of actions ΔJ_x starting from different initial amplitudes (left), and (2) the spectrum obtained from turn-by-turn trajectory data $\bar{x} \pm i\bar{p}_x$ (right). The ratio between the amplitudes of the two leading harmonics $\frac{A_2}{A_1}$ is the objective used to minimize the orbit tune diffusion.

technique [16]. By tuning the nonlinear knobs, the ratio between the two leading harmonics $r = \frac{A_2}{A_1}$ was minimized as shown in the right subplot in Fig. 2. As a consequence, the smaller amplitude components were also suppressed. Note that this procedure is performed independently for several initial conditions of varying amplitude. As a result, the tune diffusion of each particle is suppressed, but the tunes may be amplitude-dependent. The same procedure is repeated for the vertical plane.

Since we want to minimize the fluctuations of four different quantities with different initial conditions simultaneously, the construction of such a nonlinear lattice becomes a typical multi-objective optimization problem: given a set of nonlinear knobs K_i within their allowed ranges; subject to some constraints, such as certain desired chromaticities; simultaneously minimize four objective functions, i.e., $\frac{\Delta J_{x,y}}{J_{x,y}}$ and $r_{x,y}$ of multi-particles launched from different initial conditions. The Nondominated sorting genetic algorithm-II [17] was used to implement the optimization.

Thus far, we have only discussed uncoupled linear lattices. When linear coupling is present, a different parameterization, such as the one described in [18], is needed.

APPLICATIONS

We applied this method to optimize a nonlinear DBA lattice for the NSLS-II main storage ring, which is presently in operation, and a under-design hybrid-MBA candidate lattice for the future upgrade.

Double-Bend Achromat

NSLS-II [19] is a dedicated 3rd generation medium energy (3 GeV) light source operated by BNL. The storage ring's lattice is a typical DBA structure. In this configuration, three families of chromatic sextupoles are used to correct its chromaticity to +7. Then six families of harmonic sextupoles in dispersion-free sections are used as tuning knobs.

Below we present the nonlinear lattice performance of an optimized solution using the tracking simulation code ELEGANT [20]. Figure 3 illustrates the on-momentum DA (through 1,024 turns of particle tracking). Each stable initial

condition is colored with the tune diffusion rate (over 1,024 turns) obtained using the NAFF technique.

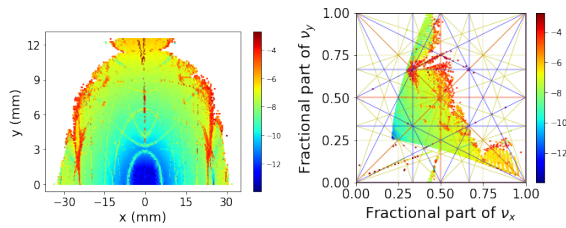


Figure 3: DA of the DBA lattice observed at the center of the long straight section (left). Tune footprint of the DBA lattice in the tune space (right). A large amplitude-dependent tune-spread is observed, and various resonance lines can be crossed. Colors indicate the tune diffusion rate.

One of the features of an integrable system is that the trajectories are confined to tori in the phase space. This is apparent in the turn-by-turn tracking data shown in Fig. 4. Although trajectories begin to deviate from the Courant-Snyder ellipse gradually when the amplitude increases, they are still confined to deformed tori. It therefore appears that this lattice possesses two QIs whose values near the reference orbit are quantitatively close to the Courant-Snyder actions.

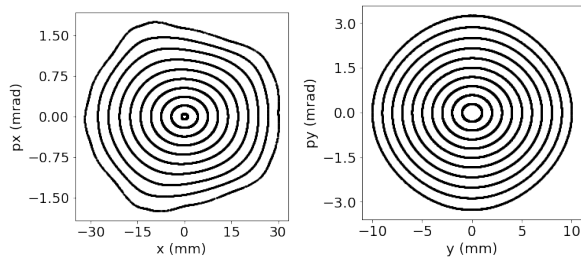


Figure 4: Simulated trajectories of the DBA lattice starting from different initial conditions in the horizontal (left) and vertical (right) phase space. Within the DA, although the trajectories deviate from the Courant-Snyder ellipse, they are still confined to thin tori.

The robustness of this lattice has been confirmed in both simulation and experiment. After adding various realistic errors to the magnets in the simulation, a sufficient DA for off-axis injection still remains. This lattice has been successfully commissioned at NSLS-II by modifying the sextupole configuration. Compared with the nominal NSLS-II lattice, the required bunch-by-bunch feedback amplitude gain for this nonlinear lattice is reduced by 50% and 75% in the horizontal and vertical planes, respectively (in the case of 400 mA stored beam current). This appears to be due to the increased chromaticity and nonlinear tune-spread.

Multi-Bend Achromat

Currently various MBA-type lattices already reach diffraction-limited horizontal emittances to deliver much brighter X-ray beams. Like the DBA case, it is interesting to explore whether it is possible to design a nonlinear

MBA lattice with two QIs. An ESRF-EBS type hybrid 7BA lattice [21] is being considered as one of the options for the future NSLS-II upgrade. A two-stage optimization has been implemented on it. First, the settings of the chromatic and harmonic sextupoles were optimized to correct the chromaticities, to minimize the fluctuations of the Courant-Snyder actions, and to maximize the ratio of the two leading harmonics. After this procedure, four octupoles inside the dispersive bumps were optimized to further minimize these objectives. The resulting DA and trajectories in the phase space are shown in Figs. 5 and 6.

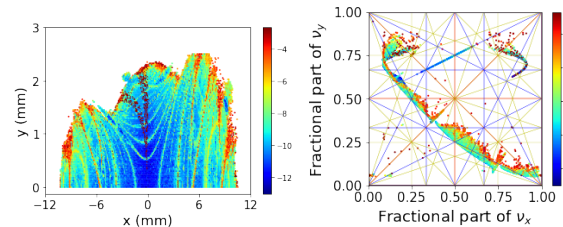


Figure 5: (Color) DA of the MBA lattice in the transverse $x - y$ plane colored with the tune diffusion rate. A large amplitude-dependent tune-spread is observed in the MBA lattice constructed with QIs.

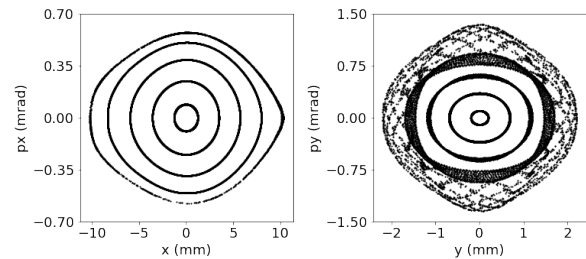


Figure 6: Simulated trajectories of the MBA lattice in the horizontal (left) and vertical (right) phase space. The vertical trajectories begin to smear out from thin tori gradually, but some patterns are visible.

SUMMARY

We demonstrated that a conventional DBA or MBA lattice can be retuned to possess two approximate invariants by optimizing the settings of only the sextupoles and octupoles. The resulting DA is large (but finite), most particle trajectories are regular and confined to tori, and the amplitude-dependent betatron tunes are well-defined and stable. Similar to a lattice such as IOTA, a large nonlinear tune-spread exists that can provide enhanced Landau damping.

ACKNOWLEDGMENTS

We would like to thank L-H. Yu, M. Borland, R. Lindberg, Y-P. Sun, Y. Hao, E. Stern, A. Valishev, A. Romanov, N. Kuklev and G. Xu for the stimulating and collaborative discussions.

REFERENCES

- [1] S. Antipov *et al.*, “IOTA (Integrable Optics Test Accelerator): facility and experimental beam physics program”, *Journal of Instrumentation*, vol. 12, no. 03, p. T03002, Mar. 2017. doi:10.1088/1748-0221/12/03/t03002
- [2] V. Danilov, “Practical solutions for nonlinear accelerator lattice with stable nearly regular motion”, *Physical Review Special Topics - Accelerators and Beams*, vol. 11, p. 114001, Nov. 2008. doi:10.1103/physrevstab.11.114001
- [3] V. Danilov and S. Nagaitsev, “Nonlinear accelerator lattices with one and two analytic invariants”, *Physical Review Special Topics - Accelerators and Beams*, vol. 13, p. 084002, Aug. 2010. doi:10.1103/physrevstab.13.084002
- [4] K. Ruisard *et al.*, “Single-invariant nonlinear optics for a small electron recirculator”, *Physical Review Special Topics - Accelerators and Beams*, vol. 22, p. 041601, Apr. 2019. doi:10.1103/physrevaccelbeams.22.041601
- [5] A. Dragt, Dynamical Systems and Accelerator Theory Group, <https://www.physics.umd.edu/dsat/dsatliemethods.html>
- [6] A. Chao, *Physics of Collective Beam Instabilities in High Energy Accelerators*, New York, USA: Wiley, 1993.
- [7] E. Stern, “Suppression of Instabilities Generated by an Anti-Damper with a Nonlinear Magnetic Element in IOTA”, FNAL, Batavia, IL, Rep. FERMI LAB-CONF-18-132-APCD, 2018.
- [8] L-H. Yu, “Analysis of nonlinear dynamics by square matrix method”, *Physical Review Special Topics - Accelerators and Beams*, vol. 20, p. 034001, Mar. 2017. doi:10.1103/PhysRevAccelBeams.20.034001
- [9] Y. P. Sun and M. Borland, “Comparison of Nonlinear Dynamics Optimization Methods for APS-U”, in *Proc. North American Particle Accelerator Conf. (NAPAC'16)*, Chicago, IL, USA, Oct. 2016, pp. 924-927. doi:10.18429/JACoW-NAPAC2016-WEPOB15
- [10] M. Borland, private communication, 2017.
- [11] J. Liouville, “Note sur l’intégration des équations différentielles de la Dynamique, présentée au Bureau des Longitudes le 29 juin 1853”, *Journal de Mathématiques pures et appliquées*, vol. 20, pp. 137–138, 1855.
- [12] V. Arnold, *Mathematical Methods of Classical Mechanics*, New York: Springer-Verlag, 1989.
- [13] E. Courant and H. Snyder, “Theory of the alternating-gradient synchrotron”, *Annals of Physics*, vol. 281, pp. 360-408, 1958. doi:10.1006/aphy.2000.6012
- [14] H. Yoshida, “Construction of higher order symplectic integrator”, *Physics Letters A*, vol. 150, pp. 262–268, Nov. 1990. doi:10.1016/0375-9601(90)90092-3
- [15] A. Chao, “Lecture Notes on Topics in Accelerator Physics”, SLAC National Accelerator Lab., Menlo Park, CA, USA, Rep. SLAC-PUB-9574, Nov. 2002.
- [16] J. Laskar, “Frequency Map Analysis and Particle Accelerators”, in *Proc. 20th Particle Accelerator Conf. (PAC'03)*, Portland, OR, USA, May 2003, paper WOAB001, pp. 378-382.
- [17] K. Deb, *Multi-Objective Optimization Using Evolutionary Algorithms*, New York, USA: Wiley, 2001.
- [18] D. A. Edwards and L. C. Teng, “Parametrization of linear coupled motion in periodic systems”, *IEEE Transactions on nuclear science*, vol. 20, no. 3, pp. 885–888, 1973. doi:10.1109/tns.1973.4327279
- [19] National Synchrotron Light Source II, <https://www.bnl.gov/ns1s2/project/PDR/>.
- [20] M. Borland *et al.*, “ELEGANT: A Flexible SDDS-Compliant Code for Accelerator Simulation”, Argonne National Lab., Lemont, IL, USA, Rep. LS-287, 2000.
- [21] L. Farvacque *et al.*, “A Low-Emittance Lattice for the ESRF”, in *Proc. 4th Int. Particle Accelerator Conf. (IPAC'13)*, Shanghai, China, May 2013, paper MOPEA008, pp. 79-81.